iScience

CellPress
OPEN ACCESS

Article

Quantitative analysis of asynchronous transcription-translation and transcription processivity in *Bacillus subtilis* under various growth conditions

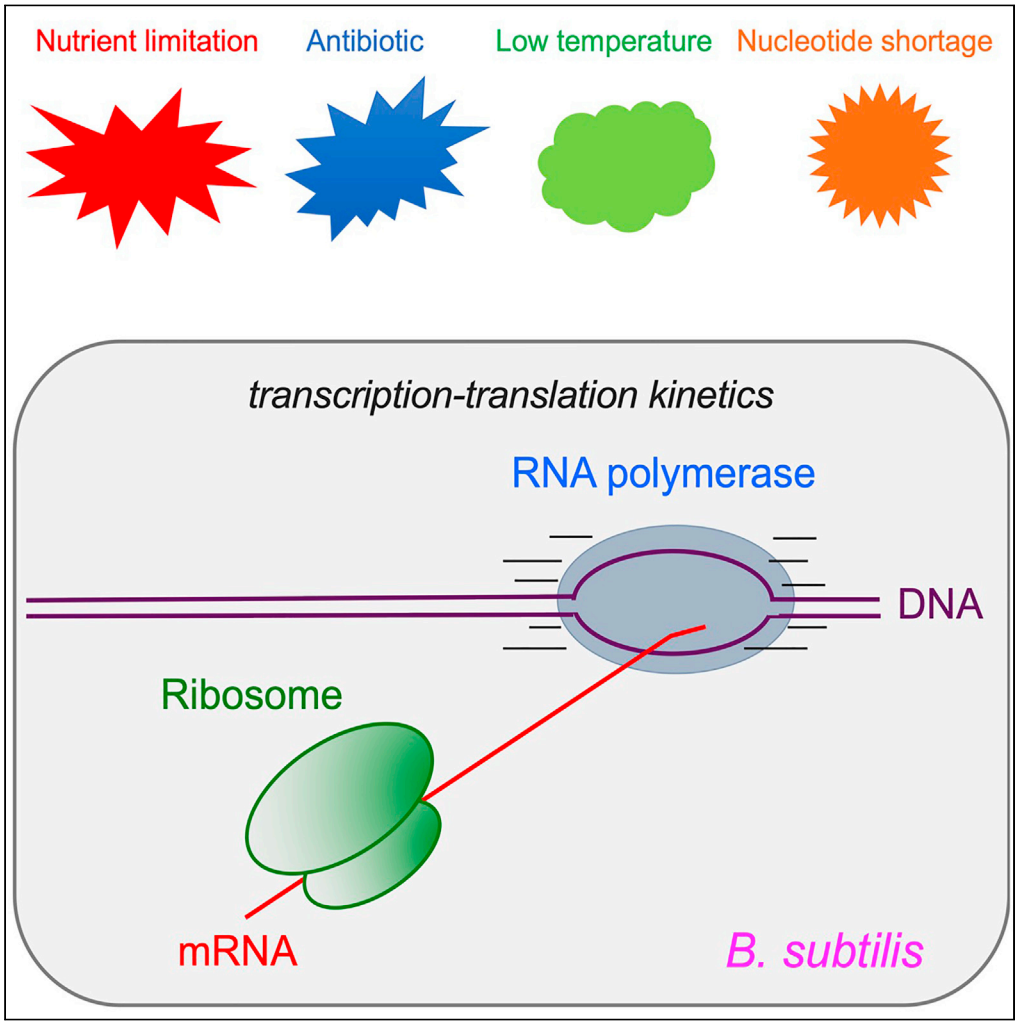

Manlu Zhu, Haoyan Mu, Fei Han, Qian Wang, Xiongfeng Dai

zhumanlu@mail.ccnu.edu.cn (M.Z.)
daixiongfeng@mail.ccnu.edu.cn (X.D.)

Highlights

Asynchronous Transcription-Translation in *B. subtilis* under various growth conditions

Loss of transcription processivity occurs constitutively in several genes/operons

Lack of Rho-mediated translation control of transcription kinetics in *B. subtilis*

Transcription processivity is affected by the transcription elongation speed

Zhu et al., iScience *24*, 103333
November 19, 2021
https://doi.org/10.1016/j.isci.2021.103333

iScience

CellPress
OPEN ACCESS

Article

Quantitative analysis of asynchronous transcription-translation and transcription processivity in *Bacillus subtilis* under various growth conditions

Manlu Zhu,[1,*] Haoyan Mu,[1] Fei Han,[1,2] Qian Wang,[1,2] and Xiongfeng Dai[1,3,*]

SUMMARY

Tight coordination between transcription and translation has long been recognized as the hallmark of gene expression in bacteria. In *Escherichia coli* cells, disruption of the transcription-translation coordination leads to the loss of transcription processivity via triggering Rho-mediated premature transcription termination. Here we quantitatively characterize the transcription and translation kinetics in Gram-positive model bacterium *Bacillus subtilis*. We found that the speed of transcription elongation is much faster than that of translation elongation in *B. subtilis* under various growth conditions. Moreover, a Rho-independent loss of transcription processivity occurs constitutively in several genes/operons but is not subject to translational control. When the transcription elongation is decelerated under poor nutrients, low temperature, or nucleotide depletion, the loss of transcription processivity is strongly enhanced, suggesting that its degree is modulated by the speed of transcription elongation. Our study reveals distinct design principles of gene expression in *E. coli* and *B. subtilis*.

INTRODUCTION

It is widely accepted that, in *E. coli* cells, transcription and translation process are tightly coordinated where the lead ribosome closely follows RNA polymerase (RNAP) during gene expression (McGary and Nudler, 2013; Miller et al., 1970). Specially, the speeds of transcription and translation elongation are synchronized in bacterial cells under various nutrient conditions, enabling the full processivity of transcription (Iyer et al., 2018; Proshkin et al., 2010; Vogel and Jensen, 1994b; Zhu et al., 2019). A series of recent biochemical and structural studies have provided evidences that such coordination is mediated by the physical coupling between RNAP and the lead ribosome(Burmann et al., 2010; Demo et al., 2017; Kohler et al., 2017; O'Reilly et al., 2020; Saxena et al., 2018; Wang et al., 2020; Webster et al., 2020). Alternative models such as the stochastic coupling model have also been proposed (Chen and Fredrick, 2018; Rui et al., 2016). In addition, it has been found that alternative factors such as (p)ppGpp assist the kinetic coordination between transcription and translation (Iyer et al., 2018; Kingston et al., 1981; Vogel and Jensen, 1994a; Vogel et al., 1992; Zhu et al., 2019).

It has been well established that disruption of transcription-translation coordination, by, e.g., nonsense mutation or antibiotic treatment, leads to Rho-mediated premature transcription termination (PTT), a loss of transcription processivity (Adhya and Gottesman, 1978; Newton et al., 1965; Zhu et al., 2019). Such mechanism suppresses persuasive transcription during transcription-translation dissociation so that the cellular investments on transcription and translation are coordinated (Richardson, 1991, 2003). It could also function in limiting the expression of deleterious foreign DNA (e.g., phage-related or xenogenic DNA) (Aleksandra et al., 2016). Rho-mediated control of transcription processivity could significantly affect the gene expression process (exemplified in the polarity phenomenon) (Adhya and Gottesman, 1978; Newton et al., 1965) and fundamental physiological processes of bacterial cells (Aleksandra et al., 2016).

The notion of Rho-mediated loss of transcription processivity during transcription-translation dissociation, although firmly established in *E. coli*, is not necessarily applicable to other bacterial species. For example, previous studies have shown that Rho factor has a diminished role in the Gram-positive bacterium *B. subtilis*, as reflected by (1) Rho factor is dispensable in *B. subtilis*, whereas it is essential in *E. coli* (Ingham et al., 1999; Quirk et al., 1993; Vladimir et al., 2017; Yakhnin et al., 2001); (2) the majority of terminators in

[1]Hubei Key Laboratory of Genetic Regulation and Integrative Biology, School of Life Sciences, Central China Normal University, Wuhan, Hubei Province, China

[2]These authors contributed equally

[3]Lead contact

*Correspondence: zhumanlu@mail.ccnu.edu.cn (M.Z.), daixiongfeng@mail.ccnu.edu.cn (X.D.)

https://doi.org/10.1016/j.isci.2021.103333

B. subtilis are intrinsic terminators, and Rho-dependent terminators are rare (De Hoon et al., 2005; Naville and Gautheret, 2009). A very recent study has reported that, in contrast to the tight transcription-translation coordination in *E. coli*, RNAP outpaces the lead ribosomes in *B. subtilis* cells grown in rich medium, providing a functional explanation on the diminished role of Rho-dependent transcription termination in *B. subtilis* (Johnson et al., 2020).

Since Rho-mediated loss of transcription processivity is a consequence of the transcription-translation dissociation in *E. coli*, the observation of transcription-translation dissociation of *B. subtilis* in rich medium poses several important questions: What is the status of transcription processivity in *B. subtilis*? How is it regulated, and is it also subject to Rho-mediated translational control? Moreover, considering that *B. subtilis* cells frequently encounter various stressful conditions in their natural niches (soil) (Gray et al., 2019; Van Dijl and Hecker, 2013), it remains undetermined whether and how transcription-translation interplay and transcription processivity are affected by stress. Here we quantitatively characterize the transcription and translation kinetics in *B. subtilis* under a broad range of growth conditions. We confirm the dissociation status between translation and transcription under various growth conditions in *B. subtilis*. In particular, we identify that the loss of transcription processivity occurs constitutively during transcription-translation dissociation. In addition, it is Rho independent and is not subject to translational control and instead is mainly affected by the elongation speed of RNAP.

RESULTS

Asynchronous transcription and translation in *B. subtilis*

We first focused on the *B. subtilis* 168 strain exponentially growing in glycerol plus casamino acid (gly + cAA) medium (a rich medium supporting a doubling time of 29 min). To quantitatively measure the transcription kinetics, we applied our recently established multiple-probes qRT-PCR method based on the *lacZ* induction system of *E. coli* (Zhu et al., 2019). To adapt this approach to *B. subtilis*, we integrated a xylose-inducible *xylR-PxylA-lacZ* cassette into the chromosome of *B. subtilis* (Figure 1A, left). In this case, the transcription of *lacZ* mRNA in *B. subtilis* could be induced by xylose and be further measured by qRT-PCR. Since *lacZ* is an exogenous gene for *B. subtilis*, we also focused on the transcription of the native *araAB* mRNA that is inducible by arabinose (Figure 1A, right) (Sá-Nogueira et al., 1997).

For both *lacZ* and *araAB* mRNA, we used three pairs of qRT-PCR primers to detect the induction kinetics of different mRNA sub-regions, the head (detected by P297 for *lacZ*; ara130 *for araAB)*, the middle (detected by P1578 for *lacZ*; ara1477 for *araAB*), and the tail (detected by P3105 for *lacZ*; ara3141 for *araAB*) (Figure 1A, Figure S1). As exemplified in Figures 1B and 1C, both the *lacZ* and *araAB* mRNA abundance are linearly correlated with the time following the addition of inducers. From the linear induction curve of each pair of primers, we could deduce the transcription time of each mRNA sub-regions (T_{head}, T_{mid}, T_{tail}) and further obtain the transcription elongation rate of RNAP (see STAR method section). We found that the transcription elongation rates of *lacZ* mRNA and *araAB* mRNA in *B. subtilis* were similar to each other, at a value of ~25–26 codons/s (75–80 nt/s) (Figure 1D) with a high reproducibility (Figure S2). This value is much higher than that of *E. coli* cells, ~16 codons/s (Zhu et al., 2019) and is consistent with the report of Johnson *et al.* (2020).

We next measured the induction kinetics of LacZ protein in order to investigate the potential interplay between transcription and translation. As shown in Figure 1E, the time required to transcribe the complete *lacZ* mRNA was significantly shorter than that required to translate the complete LacZ protein, indicating that transcription is naturally dissociated from translation in *B. subtilis*. This result is consistent with the recent report of Johnson *et al.*, which was also done in nutrient-rich medium (Johnson et al., 2020). Quantitatively, the speed of transcription elongation (~25 codon/s) is 65% higher than that of translation elongation (~15 aa/s) in *B. subtilis*, whereas these two values are equal in *E. coli* (Figure 1F) (Zhu et al., 2019).

Rho-independent loss of transcription processivity in *B. subtilis*

An important parameter of transcription kinetics is the transcription processivity, which is affected by the degree of PTT (Iyer et al., 2016). A loss of transcription processivity means that an elongating RNA polymerase fails to reach the 3′ end of an operon to generate a full-length transcript (Iyer et al., 2016). It could mechanistically originate from various mechanisms such as the Rho-mediated form occurring when transcription-translation coordination is disrupted in *E. coli* (Iyer et al., 2018; Zhu et al., 2019) or a permanent arrest of transcription in cases such as treating cells with a transcription blocker such as

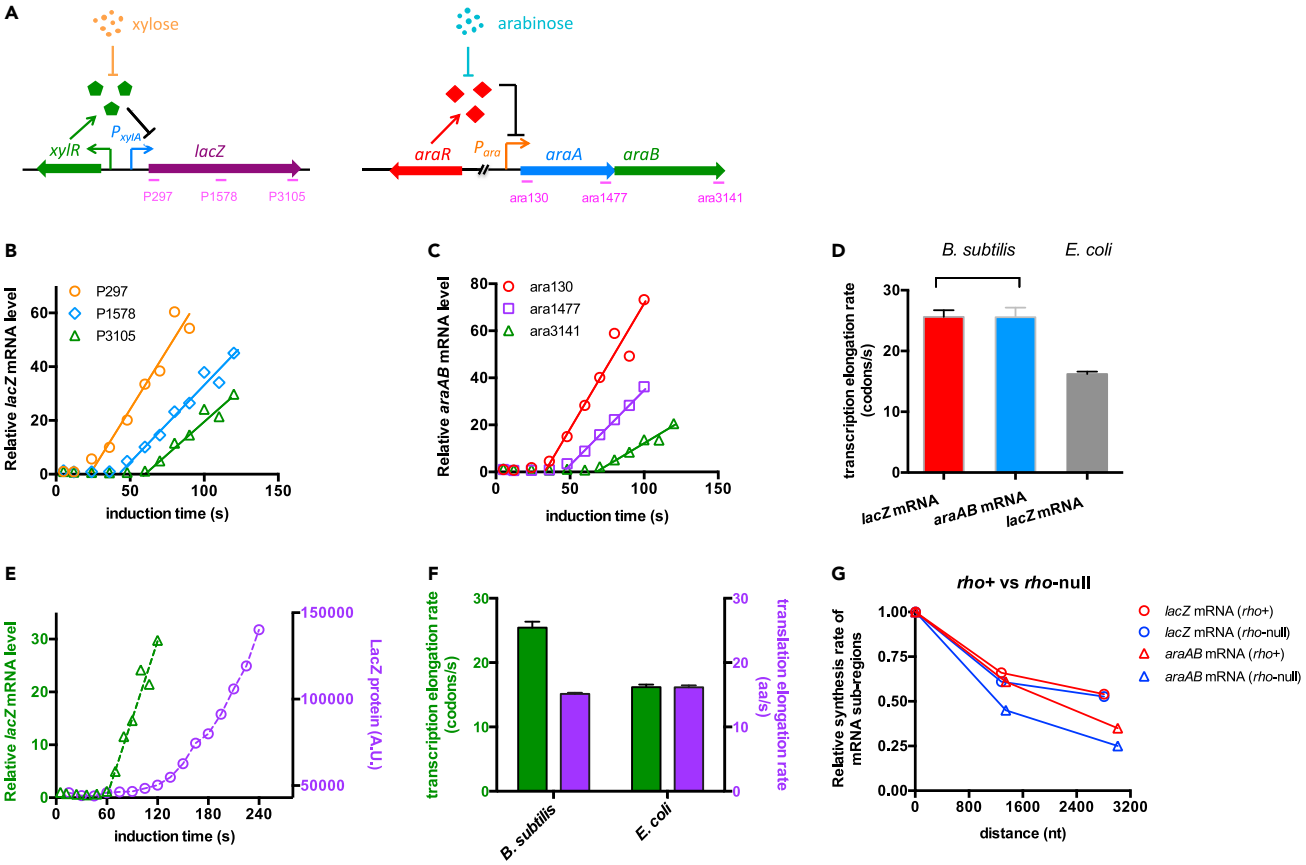

Figure 1. Characterization of transcription and translation kinetics of *Bacillus subtilis*

Cells were grown in glycerol plus casamino acid (gly + cAA) medium.

(A) Two inducible systems used in this study. A *xylR-PxylA-lacZ* cassette was integrated into the *lacA* locus of *B. subtilis* genome. The expression of *lacZ* gene is controlled by the XylR repressor and thus is induced by xylose. The other inducible system is the native *ara* operon of *B. subtilis*, which is controlled by AraR and is induced by arabinose. We focused on the *araAB* region of the *ara* operon. Regions detected by three qRT-PCR primers are labeled in pink.

(B) The induction kinetics of the *lacZ* mRNA. Three pairs of primers were used to detect the abundances of *lacZ* mRNA sub-regions. The rising part of each induction curve was fitted to a linear line.

(C) The induction kinetics of *araAB* mRNA detected by three pairs of qRT-PCR primers, being similar to (B)

(D) The transcription elongation rates of both *B. subtilis* and *E. coli*. Data of *E. coli lacZ* mRNA are from Zhu et al (2019). Data are represented as mean ± SD.

(E) The induction curve of the intact *lacZ* mRNA (detected by P3105, green triangles) is plotted together with the induction curve of LacZ protein (purple circles).

(F) The transcription and translation elongation rates of *B. subtilis* and *E. coli*. Data of *E. coli* cells are from Zhu et al (2019). Data are represented as mean ± SD.

(G) The transcription processivity of *lacZ* mRNA and *araAB* mRNA in both *rho*$^+$ (red symbols) and *rho*-null strains (blue symbols) of *B. subtilis*. The relative accumulation rates of mRNA sub-regions (slope of the linear induction curve in B and C) are plotted against the hybridization locations of primers in *lacZ* or *araAB* mRNA. The detection positions of the 5′ primer (P297 for *lacZ* mRNA and ara130 for *araAB* mRNA) were set as location "zero" (x axis). The accumulation rates of the 5′ mRNA sub-regions detected by P297 or ara130 were set as "1" (y axis).

actinomycin D (Levinthal and Higa, 1962; Miller, 1987). Since translation is naturally dissociated from transcription in *B. subtilis*, we wondered the status of transcription processivity in such cases. The slope of the linear transcriptional induction curve (Figures 1B and 1C) denotes the relative accumulation rate of each mRNA sub-region (head, middle and tail regions) (Iyer et al., 2016; Zhu et al., 2019). Comparing the slope of the head and tail region is a reliable and standard approach to quantify the processivity of RNAP during transcription elongation given that the stabilities of different mRNA sub-regions are almost the same as each other (Figure S3) (Iyer et al., 2016, 2018; Vogel et al., 1992; Zhu et al., 2019). As shown in Figure 1G, we found that the mRNA accumulation rate significantly decreased from 5′ to 3′ direction for both *lacZ* and *araAB* mRNA (red circles and triangles), suggesting a significant loss of transcription processivity. Quantitatively, the mRNA accumulation rates of *lacZ* and *araAB* dropped by ~40% and ~65% from the head region to tail region, respectively. The loss of transcription processivity

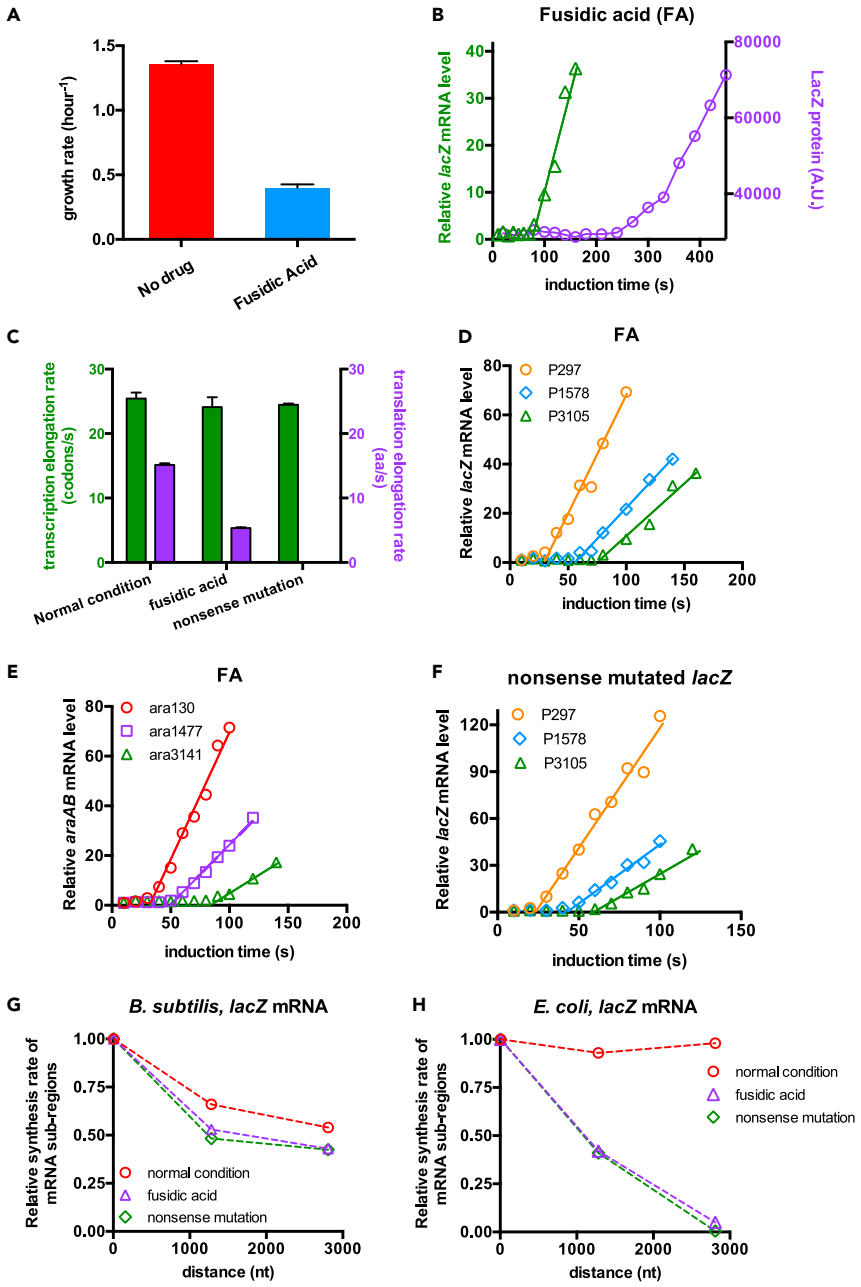

Figure 2. Transcription and translation kinetics of *B. subtilis* following fusidic acid (FA) treatment and nonsense mutation

Cells were grown in gly + cAA medium.

(A) THE growth rates of *B. subtilis* in gly + cAA medium supplemented with/without 0.2 μg/mL FA. Data are represented as mean ± SD.

(B) The induction curve of the complete *lacZ* mRNA (green triangles) and LacZ protein (purple circles) for *B. subtilis* grown in gly + cAA medium supplemented with 0.2 μg/mL FA.

(C) Summary of the transcription and translation elongation rates of *lacZ* mRNA for *B. subtilis*0020 under normal condition, FA treatment, and nonsense mutation. Data are represented as mean ± SD.

(D) The induction kinetics of the *lacZ* mRNA for *B. subtilis* under FA treatment.

(E) The induction kinetics of the *araAB* mRNA for *B. subtilis* under FA treatment.

(F) The induction kinetics of a nonsense-mutated *lacZ* mRNA. The coding sequence of the 154th amino acid residue of the native *lacZ*, "TGG," was mutated to "TAA" stop codon.

Figure 2. *Continued*

(G) The transcription processivity of *lacZ* mRNA in *B. subtilis* under normal condition, FA treatment, and nonsense mutation. The same as Figure 1G, the relative accumulation rates of mRNA sub-regions (slope of the linear induction curve) are plotted against the hybridization locations of primers for *lacZ* mRNA. (H) The transcription processivity of *lacZ* mRNA in *E. coli* under normal condition, FA treatment, and nonsense mutation. Data originate from Zhu et al (2019).

was also observed in two additional native operons, *mtlAFD* and *xynPB* operons (Figure S4). To investigate the potential origin of the loss of transcription processivity, we next measured the transcription kinetics of *rho*-null mutant (Figure S5). If the loss of transcription processivity originates from Rho-dependent PTT in *B. subtilis*, it should be substantially alleviated in the *rho*-null strain. The growth rate of the *rho*-null mutant was mildly lower than that of wild-type cells (Figure S6), being consistent with previous reports that Rho is dispensable for *B. subtilis* (Ingham et al., 1999; Vladimir et al., 2017). However, the loss of transcription processivity was not alleviated in the *rho*-null strain relative to rho^+ strain (Figure 1G), indicating that it is Rho independent.

Lack of translational control on the transcription processivity in *B. subtilis*

We next sought to explore the potential effect of translation on transcription processivity in *B. subtilis*. We first applied fusidic acid (FA), an antibiotic that targets ribosome translocation via inhibiting EF-G recycling, to perturb the translation elongation process (Bennett and Maaloe, 1974; Seo et al., 2006). The growth rate of *B. subtilis* in gly + cAA medium dropped by 70% during treatment with 0.2 μg/mL FA (Figure 2A, DT: ~100 min). Concomitantly, the translation time of the complete LacZ protein under FA treatment became much longer than that under normal condition (purple circles in Figures 2B and 1E), suggesting a much slower translation elongation rate. As shown in Figure 2C (purple bar), the translation elongation rate of *B. subtilis* under FA treatment was only ~5 aa/s, being approximately one-third of the normal value (~15 aa/s). In contrast, the transcription elongation rate remained almost unaffected under FA treatment (Figure 2C, green bar).

Introducing nonsense mutation is another approach to investigate the effect of translation on transcription (Newton et al., 1965). We introduced a "TAA" stop codon in the upper part of *lacZ* gene and repeated the transcription kinetics of *lacZ* mRNA. Being similar to FA treatment, nonsense mutation did not affect the transcription elongation rate as well (Figure 2C, green bar). Therefore, both FA treatment and nonsense mutation significantly amplify the degree of transcription-translation dissociation in *B. subtilis*. However, analysis of the transcription kinetics (Figures 2D–2F) showed that transcription processivity was only weakly affected by FA treatment and nonsense mutation (Figures 2G and S7). In contrast, our recent quantitative study shows that FA treatment and nonsense mutation, which both disrupt the transcription-translation coordination, cause a severe loss of transcription processivity during *lacZ* mRNA induction in *E. coli* cells (Figure 2H) (Zhu et al., 2019). In summary, the degree of transcription-translation dissociation, which is known to strongly modulate the Rho-mediated PTT in *E. coli* cells, is not an important determinant of the loss of transcription processivity here observed in *B. subtilis*.

Loss of transcription processivity is more severe under poor nutrients and low temperatures

B. subtilis frequently encounters a variety of environment stressors in their natural niches (soil), including poor nutrients and suboptimal temperatures (Gray et al., 2019; Janna et al., 2005; Van Dijl and Hecker, 2013). We therefore extended the kinetics study to poor nutrient conditions and low temperatures in order to gain an insight into the impact of stress on the transcription-translation interplay. The nutrient-limited minimal medium supports much lower growth rates than gly + cAA medium (Figure 3A). Again, we found that translation remains dissociated from transcription in poor nutrients (Figures 3B and S8). However, compared with rich medium, both transcription and translation elongation rates became lower under poor nutrients (Figure 3C) and were positively correlated with growth rate (Figure 3D). We further quantified the transcription processivity by analyzing the transcription induction kinetics (Figures 3E, 3F, and S9). Strikingly, transcription processivity drops more substantially for cells under poor nutrients than their counterparts growing under rich medium (Figures 3G and 3H). In addition, the loss of transcription processivity in poor nutrient conditions was still Rho independent since its level was not reduced in the *rho*-null strains (Figures 3I and S10).

The growth rate of *B. subtilis* at a low temperature, 25°C, decreased to only ~30% of that at 37°C (subpanel in Figure 4A). Strikingly, both transcription and translation elongation rates dropped by a factor of ~3 at

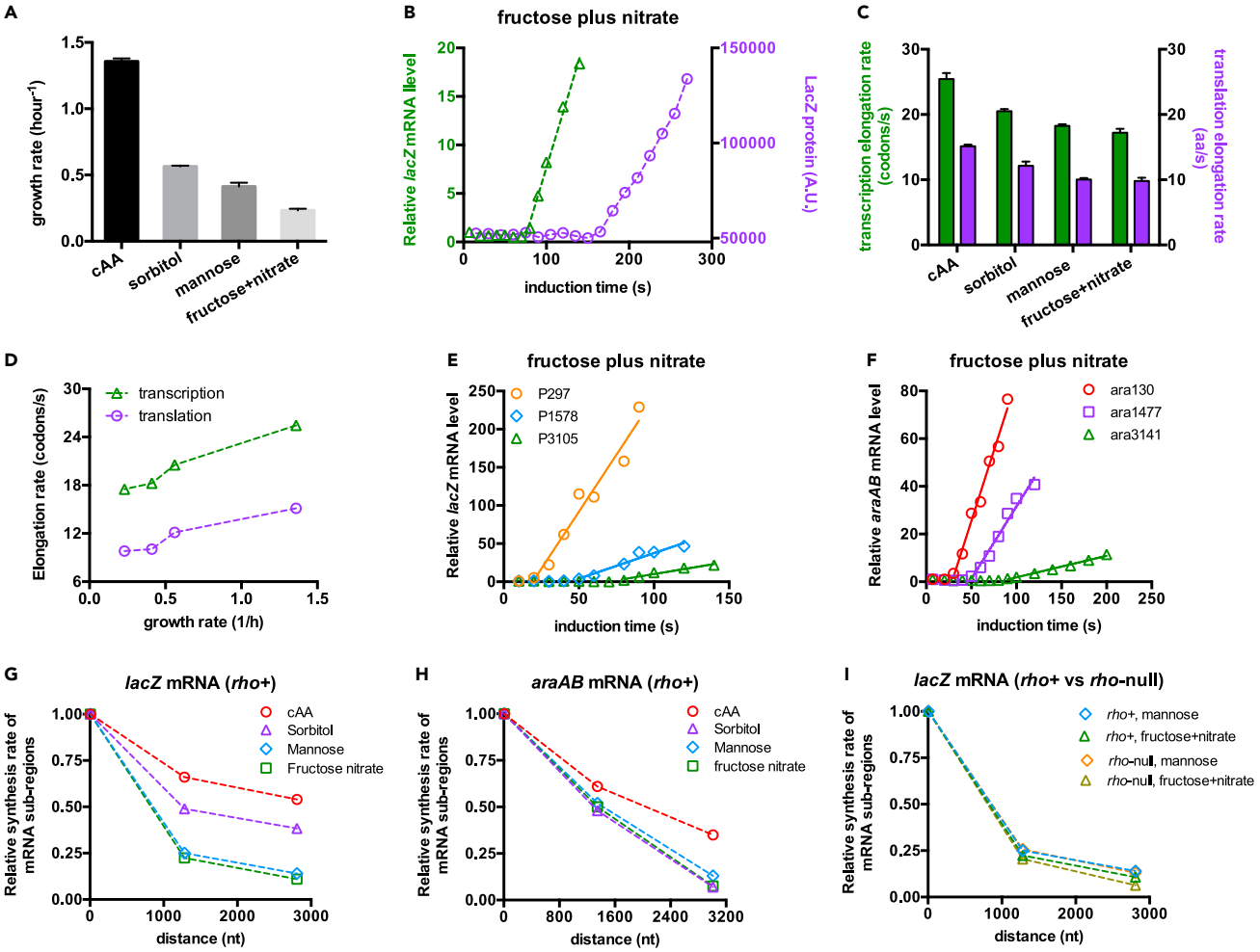

Figure 3. Transcription and translation kinetics of *B. subtilis* under poor nutrient conditions

(A) The growth rates of *B. subtilis* under different nutrient conditions. Data are represented as mean ± SD.

(B) The induction curves of the intact *lacZ* mRNA (green triangles) and LacZ protein (purple circles) for *B. subtilis* grown in a poor nutrient condition, fructose plus nitrate medium, which supports a doubling time of ~3 h.

(C) Summary of transcription (green bar) and translation (purple bar) elongation rates of *B. subtilis* under different nutrient conditions. Data are represented as mean ± SD.

(D) Growth rate-dependent transcription and translation elongation rates under different nutrient conditions. Data of growth rates are from (A) Data of transcription and translation elongation rates are from (C)

(E) The induction kinetics of *lacZ* mRNA in *B. subtilis* grown in fructose plus nitrate medium.

(F) The induction kinetics of *araAB* mRNA in *B. subtilis* grown in fructose plus nitrate medium.

(G) The transcription processivity of *lacZ* mRNA in *B. subtilis* (rho^+) under different nutrient conditions.

(H) The transcription processivity of *araAB* mRNA in *B. subtilis* (rho^+) under different nutrient conditions.

(I) The transcription processivity of *lacZ* mRNA in both rho^+ and *rho*-null strains of *B. subtilis* under mannose medium and fructose plus nitrate medium.

25°C (Figure 4A), and therefore, transcription and translation were still dissociated from each other (Figure 4B). From the induction kinetics of both *lacZ* and *araAB* mRNA (Figures 4C and 4D), we found that the loss of transcription processivity of both rho^+ and *rho*-null strains at 25°C became more marked than that at 37°C (compare circles and triangles in Figures 4E and 4F), being similar to the case of nutrient limitation. Moreover, the *rho*-null mutant exhibited an even stronger loss of transcription processivity than rho^+ strain at 25°C (compare red and purple triangles in Figures 4E and 4F; also see induction kinetics in Figure S11). In summary, being different from the cases of fusidic acid and nonsense mutation (Figure 2), the status of transcription processivity depends strongly on the nutrient quality and temperature, implying that it is controlled by factors other than transcription-translation dissociation.

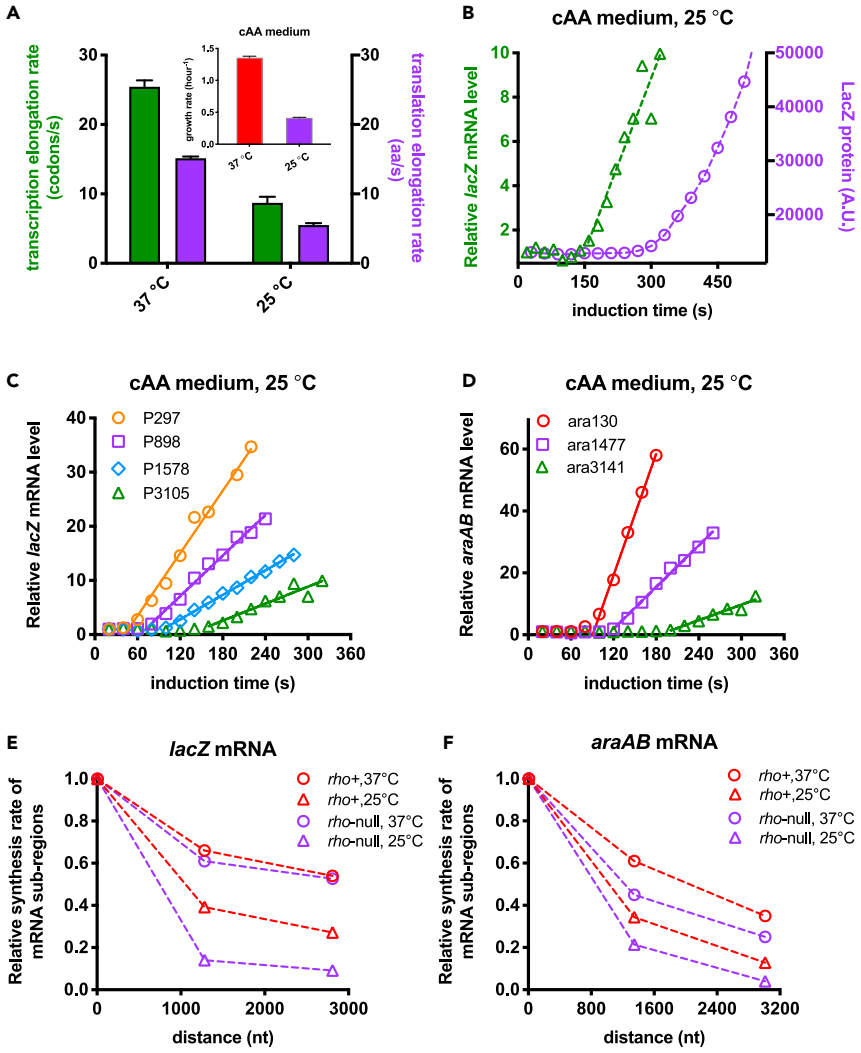

Figure 4. Transcription and translation kinetics of *B. subtilis* at 25°C

B. subtilis cells were grown in gly + cAA medium.

(A) The transcription and translation elongation rates of *B. subtilis* under 37°C and 25°C. Data of the growth rate are shown in the subpanel. Data are represented as mean ± SD.

(B) The induction curves of the intact *lacZ* mRNA and LacZ protein for *B. subtilis* at 25°C.

(C) The induction kinetics of *lacZ* mRNA in *B. subtilis* at 25°C.

(D) The induction kinetics of *araAB* mRNA in *B. subtilis* at 25°C.

(E) The transcription processivity of *lacZ* mRNA for both *rho*$^+$ and *rho*-null strains of *B. subtilis* at two temperatures.

(F) The transcription processivity of *araAB* mRNA for both *rho*$^+$ and *rho*-null strains of *B. subtilis* at two temperatures.

Loss of transcription processivity is more severe during deceleration of transcription elongation

Given that the transcription elongation rate decreases under both poor nutrients and low temperatures, the more substantially compromised transcription processivity could simply be due to a further slowdown of RNAP movement as increased pauses of RNAP could create more windows of time for the occurrence of an RNAP drop-off and transcriptional termination event, further resulting in the loss of processivity (Ray-Soni et al., 2016). To test this hypothesis, we sought to investigate whether directly perturbing the transcription elongation rate could affect the transcription processivity in rich medium. We applied 6-azauracil (6-aza), a drug that depletes intracellular nucleotide pools (especially UTP and GTP) of microorganisms (Exinger and Lacroute, 1992; Ishiguro et al., 2000; Lopez et al., 1979), to inhibit the transcription elongation of RNAP (illustrated on Figure 5A). As expected, addition of

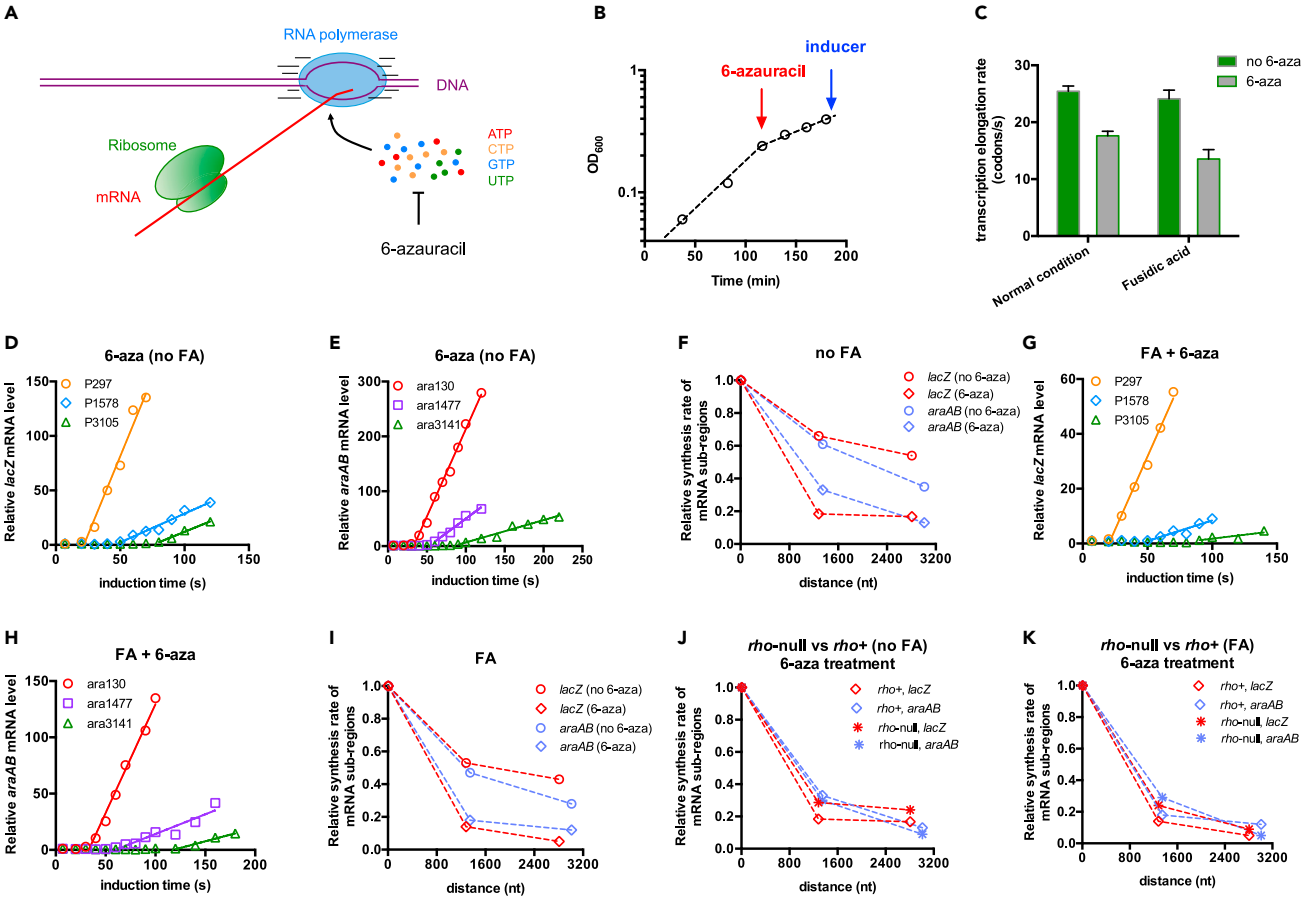

Figure 5. Transcription kinetics of *B. subtilis* treated with 6-azauracil (6-aza)

B. subtilis cells were grown in gly + cAA medium.

(A) 6-Aza was used to perturb the transcription elongation process of *B. subtilis* through depleting the cellular nucleotides pools.

(B) The growth of *B. subtilis* treated with 6-aza. Cells were first exponentially grown in gly + cAA medium to OD_{600}~0.25. 6-Aza, 500 μg/mL, was then added to deplete the cellular nucleotides pools. The cell culture was further incubated for 1 h before measuring transcription kinetics.

(C) The effect of 6-aza on the transcription elongation rate of *B. subtilis*. Cells were grown in gly + cAA medium supplemented with/without 0.2 μg/mL FA. Data are represented as mean ± SD.

(D) and (E) The induction kinetics of *lacZ* mRNA and *araAB* mRNA in *B. subtilis* treated with 6-aza. FA was not supplemented in this case.

(F) Comparison of the transcription processivities of *lacZ* (red) and *araAB* (light purple) mRNA in *B. subtilis* (*rho*$^+$ strain) with (diamond)/without (circle) 6-aza treatment. FA was not supplemented in this case.

(G) and (H) The induction kinetics of *lacZ* mRNA and *araAB* mRNA in *B. subtilis* treated with 6-aza. Being different from D and E, cells were grown with 0.2 μg/mL FA. The growth curve is shown in Figure S12.

(I) Comparison of the transcription processivities of *lacZ* (red) and *araAB* (light purple) mRNA in *B. subtilis* (*rho*$^+$ strain) with (diamond)/without (circle) 6-aza treatment. Cells were grown with 0.2 μg/mL FA.

(J) and (K) Comparison of the transcription processivities of *rho*$^+$ strain and *rho*-null strain during 6-aza treatment.

6-aza caused rapid slowdown of cell growth and decelerated the transcription elongation process (Figures 5B and 5C). Strikingly, the loss of transcription processivity is indeed enhanced by 6-aza treatment (Figures 5D and 5E), as quantitively displayed in Figure 5F. To remove any potential interference from translation, we also repeated the 6-aza experiment in medium supplementing FA (Figure S12), where the ribosome is far away behind RNAP (Figures 2B and 2C). The loss of transcription processivity also became much more marked by 6-aza treatment in this case, as shown in Figure 5I (also see induction kinetics in Figures 5G and 5H). In addition, the stronger loss of transcription processivity under 6-aza treatment was also not related to Rho factor (Figures 5J, 5K, and S13). Taken together, the above results support that the elongation rate of RNAP is an important determinant of the transcription processivity in *B. subtilis*.

DISCUSSION

In *E. coli*, the tight transcription-translation coordination effectively suppresses Rho-mediated premature transcription termination, guaranteeing the full processivity of transcription in cells under different nutrient conditions (Iyer et al., 2018; Zhu et al., 2019). Rho-mediated premature transcription termination (PTT) strongly occurs under special conditions such as nonsense mutation or treating cells with translation-blocking antibiotics (Adhya and Gottesman, 1978; Zhu et al., 2019), further substantially compromising the transcription processivity. Therefore, the transcription processivity of *E. coli* is strongly affected by the degree of transcription-translation dissociation. Being different from the scenario of *E. coli*, here we show that translation and transcription are naturally uncoordinated in *B. subtilis* under various growth conditions. Of importance, notable loss of transcription processivity occurs constitutively even in nutrient-rich medium. However, in contrast to the case of *E. coli*, it is Rho independent and does not subject to translational control and likely depends on the elongation speed of RNAP. The loss of transcription processivity is naturally attributed to the occurrence of PTT of RNAP. Given that the way of transcription termination in bacteria falls into two major categories: Rho-dependent termination and Rho-independent intrinsic termination (Aleksandra et al., 2016), the loss of transcription processivity could thus arise from intragenic Rho-independent intrinsic termination. The elongation process of transcription *in vivo* (nucleotide incorporation) is actually competitive with the process of termination (Greive and von Hippel, 2005). Studies have also shown that intrinsic termination could occur even in the absence of termination signals in which the paused/halted RNAP elongation complex could dissociate via a general forward-translocation mechanism (Santangelo and Roberts, 2004; Zhou et al., 2007). Therefore, transcription termination could occur prematurely within a gene/operon given that pausing is frequent *in vivo* (Larson et al., 2014) and can serve to halt RNAP. Recent systematic studies have also shown that there are many intrinsic NusA- or NusG-dependent pause sites within the genome of *B. subtilis* (Mondal et al., 2016; Yakhnin et al., 2020). Following this logic, a slowdown of transcription elongation (increased frequency of pausing) under harsh environments could amplify the degree of loss of transcription processivity (Davenport et al., 2000; Yang et al., 2021; Zhou et al., 2007).

In addition, alternative factors could also affect the transcription processivity. We tested two potential candidate proteins, Rnase J and GreA since they have been shown to participate in rescuing and liberating stalled/backtracked RNAP elongation complex in cases of severe transcription stalling in *B. subtilis* (Kusuya et al., 2011; Sikova et al., 2020). We found that notable loss of transcription processivity still occurs in *rnjA*-null mutant and *greA*-null mutant (Figure S14), suggesting that those two proteins do not significantly affect transcription processivity. However, an unexpected finding is that the transcription elongation speed of *rnjA*-null mutant is only half that of wild-type cells (Figure S14E), suggesting that Rnase J might be an important regulator of the transcription elongation process. This finding may provide meaningful clues for future exploration of the origin of the intriguing fast elongation speed of RNAP in *B. subtilis*.

The loss of transcription processivity could be viewed as a form of transcription attenuation by nature. In *E. coli* cells, ribosome translation plays a key role in controlling transcription attenuation, as well exemplified in the case of *trp*, *pyr* operon, and Rho-mediated polarity phenomenon (Adhya and Gottesman, 1978; Merino and Yanofsky, 2005; Turnbough, 2019). Instead, the control of transcription attenuation in *B. subtilis* mainly falls into two categories: (1) mediated by RNA-binding proteins such as TRAP and PyrR (Turnbough, 2019), as found in e.g., *typ* and *pyr* operons; (2) mediated by riboswitches (Winkler and Breaker, 2005), including tRNA-binding riboswitches (e.g., *tyrS* operon) and small-molecule binding riboswitches (e.g., *rib* operon in *B. subtilis*) (Turnbough, 2019). Given that the loss of transcription processivity here also occurred at the exogeneous *lacZ* mRNA, and therefore might not be related to those known mechanisms of transcription attenuation.

Mechanistically, the lack of Rho-mediated control of transcription processivity during transcription-translation dissociation in *B. subtilis* may be intriguing given previous reports that Rho factors from *E. coli* and *B. subtilis* share similar RNA-activated ATPase activity and *in vitro* termination efficiency on the λtR1 terminator (Ingham et al., 1999). One possible origin could lie at the Rho specificity on *rut* site. The Rho factor in *E. coli* cells does not require a specific consensus *rut* site, and its activity could be stimulated on various artificial C-rich RNA sequences and even non-C-rich RNA sequences (Hart and Roberts, 1992; Mitra and Nagaraja, 2012; Ray-Soni et al., 2016). It is possible that the activity of Rho factor in *B. subtilis* is highly sequence specific, thus being limited to only a few operons (Johnson et al., 2020).

Limitations of the study

Our results of transcription processivity are derived from a few operons. The quantitative behavior of transcription processivity could in principle be affected by both *trans*-acting protein factors that affect

transcription pausing/termination and *cis*-acting DNA elements such as intragenic anti-terminators. We expect future systematic genome-wide studies to further elucidate the status of transcription processivity among various operons in *B. subtilis*.

STAR★METHODS

Detailed methods are provided in the online version of this paper and include the following:

- KEY RESOURCES TABLE
- RESOURCE AVAILABILITY
  - Lead contact
  - Material availability
  - Data and code availability
- EXPERIMENTAL MODEL AND SUBJECT DETAILS
- METHODS DETAILS
  - Strains
  - Medium
  - Cell growth
  - Measurement of transcription kinetics
  - Measurement of mRNA degradation kinetics
  - Measurement of translation kinetics
- QUANTIFICATION AND STATISTICAL ANALYSIS

SUPPLEMENTAL INFORMATION

Supplemental information can be found online at https://doi.org/10.1016/j.isci.2021.103333.

ACKNOWLEDGMENT

We thank Professor Jianhua Zhang (Shanghai Jiao Tong University), Professor Zhemin Zhou (Jiang Nan University), and Professor Ming Sun (Central China Agricultural University) for kindly providing the *B. subtilis* 168 strain and pAX01 and pDG1730 vectors, respectively. We also greatly acknowledge Gene-Wei Li and Kurt Fredrick for useful discussions and critical reading of the manuscript during various stages of the work. This work was supported by the National Natural Science Foundation of China (31970027, 31870028, and 32022001) and by self-determined research funds of CCNU from the colleges' basic research and operation of MOE (CCNU19TS028 and CCNU20TS023).

AUTHOR CONTRIBUTIONS

Conceptualization, M.Z. and X.D.; methodology, M.Z. and X.D.; investigation, M.Z., X.D., H.M., F.H., and Q.W.; writing-original draft, M.Z. and X.D.; writing-review & editing, M.Z. and X.D.; funding acquisition, M.Z. and X.D.; resources, M.Z., H.M., and X.D.; supervision, M.Z. and X.D.

DECLARATION OF INTERESTS

The authors declare no conflict of interests.

Received: December 21, 2020
Revised: August 31, 2021
Accepted: October 20, 2021
Published: November 19, 2021

REFERENCES

Adhya, S., and Gottesman, M. (1978). Control of transcription termination. Annu. Rev. Biochem. *47*, 967–996.

Aleksandra, G.-M., Vladimir, B., Jacek, B., and Elena, B. (2016). Transcription termination factor Rho: a hub linking diverse physiological processes in bacteria. Microbiology *162*, 433–447.

Bennett, P.M., and Maaloe, O. (1974). The effects of fusidic acid on growth, ribosome synthesis and RNA metabolism in *Escherichia coli*. J. Mol. Biol. *90*, 541–561.

Burkholder, P.R., and Giles, N.H. (1947). Induced biochemical mutations in *Bacillus subtilis*. Am. J. Bot. *34*, 345–348.

Burmann, B.M., Schweimer, K., Luo, X., Wahl, M.C., Stitt, B.L., Gottesman, M.E., and Rosch, P. (2010). A NusE:NusG complex links transcription and translation. Science *328*, 501–504.

Chen, M., and Fredrick, K. (2018). Measures of single- versus multiple-round translation argue against a mechanism to ensure coupling of

transcription and translation. Proc. Natl. Acad. Sci. USA *115*, 10774–10779.

Commichau, F.M., Gunka, K., Landmann, J.J., and Stulke, J. (2008). Glutamate metabolism in Bacillus subtills: gene expression and enzyme activities evolved to avoid futile cycles and to allow rapid responses to perturbations of the system. J. Bacteriol. *190*, 3557–3564.

Dai, X., Zhu, M., Warren, M., Balakrishnan, R., Patsalo, V., Okano, H., Williamson, J.R., Fredrick, K., Wang, Y.P., and Hwa, T. (2016). Reduction of translating ribosomes enables *Escherichia coli* to maintain elongation rates during slow growth. Nat. Microbiol. *2*, 16231.

Davenport, R.J., Wuite, G.J., Landick, R., and Bustamante, C. (2000). Single-molecule study of transcriptional pausing and arrest by *E. coli* RNA polymerase. Science *287*, 2497–2500.

De Hoon, M.J.L., Makita, Y., Nakai, K., and Miyano, S. (2005). Prediction of transcriptional terminators in *Bacillus subtilis* and related species. PLoS Comput. Biol. *1*, 212–221.

Demo, G., Rasouly, A., Vasilyev, N., Svetlov, V., Loveland, A.B., Diaz-Avalos, R., Grigorieff, N., Nudler, E., and Korostelev, A.A. (2017). Structure of RNA polymerase bound to ribosomal 30S subunit. Elife *6*, e28560.

Exinger, F., and Lacroute, F. (1992). 6-Azauracil inhibition of GTP biosynthesis in *Saccharomyces cerevisiae*. Curr. Genet. *22*, 9.

Gray, D.A., Dugar, G., Gamba, P., Strahl, H., Jonker, M.J., and Hamoen, L.W. (2019). Extreme slow growth as alternative strategy to survive deep starvation in bacteria. Nat. Commun. *10*, 890.

Greive, S.J., and von Hippel, P.H. (2005). Thinking quantitatively about transcriptional regulation. Nat. Rev. Mol. Cell Biol. *6*, 221–232.

Guérout-Fleury, A., Frandsen, N., and Stragier, P. (1996). Plasmids for ectopic integration in *Bacillus subtilis*. Gene *180*, 57.

Hart, C.M., and Roberts, J.W. (1992). Rho-dependent transcription termination. Characterization of the requirement for cytidine in the nascent transcript. J. Biol. Chem. *266*, 24140–24148.

Härtl, B., Wehrl, W., Wiegert, T., Homuth, G., and Schumann, W. (2001). Development of a new integration site within the *Bacillus subtilis* chromosome and construction of compatible expression cassettes. J. Bacteriol. *183*, 2696.

Ingham, C.J., Dennis, J., and Furneaux, P.A. (1999). Autogenous regulation of transcription termination factor Rho and the requirement for Nus factors in *Bacillus subtilis*. Mol. Microbiol. *31*, 651–663.

Ishiguro, A., Nogi, Y., Hisatake, K., Muramatsu, M., and Ishihama, A. (2000). The Rpb6 subunit of fission yeast RNA polymerase II is a contact target of the transcription elongation factor TFIIS. Mol. Cell Biol. *20*, 1263–1270.

Iyer, S., Le, D., Park, B.R., and Kim, M. (2018). Distinct mechanisms coordinate transcription and translation under carbon and nitrogen starvation in *Escherichia coli*. Nat. Microbiol. *3*, 741.

Iyer, S., Park, B.R., and Kim, M. (2016). Absolute quantitative measurement of transcriptional kinetic parameters in vivo. Nucleic Acids Res. *44*, e142.

Janna, P., Marie, P., and Erland, B. (2005). Comparison of temperature effects on soil respiration and bacterial and fungal growth rates. FEMS Microbiol. Ecol. 49–58.

Johnson, G.E., Lalanne, J.B., Peters, M.L., and Li, G.W. (2020). Functionally uncoupled transcription–translation in *Bacillus subtilis*. Nature *585*, 124–128.

Kingston, R.E., Nierman, W.C., and Chamberlin, M.J. (1981). A direct effect of guanosine tetraphosphate on pausing of *Escherichia coli* RNA polymerase during RNA chain elongation. J. Biol. Chem. *256*, 2787–2797.

Kohler, R., Mooney, R.A., Mills, D.J., Landick, R., and Cramer, P. (2017). Architecture of a transcribing-translating expressome. Science *356*, 194–197.

Kusuya, Y., Kurokawa, K., Ishikawa, S., Ogasawara, N., and Oshima, T. (2011). Transcription factor GreA contributes to resolving promoter-proximal pausing of RNA polymerase in *Bacillus subtilis* cells. J. Bacteriol. *193*, 3090–3099.

Larson, M.H., Mooney, R.A., Peters, J.M., Windgassen, T., Nayak, D., Gross, C.A., Block, S.M., Greenleaf, W.J., Landick, R., and Weissman, J.S. (2014). A pause sequence enriched at translation start sites drives transcription dynamics *in vivo*. Science *344*, 1042–1047.

Levinthal, C., and Higa, K.A. (1962). Messenger RNA turnover and protein synthesis in *B. subtilis* inhibited by actinomycin D. Proc. Natl. Acad. Sci. USA *48*, 1631–1638.

Lopez, J.M., Marks, C.L., and Freese, E. (1979). The decrease of guanine nucleotides initiates sporulation of *Bacillus subtilis*. Biochim. Biophys. Acta. *587*, 238–252.

McGary, K., and Nudler, E. (2013). RNA polymerase and the ribosome: the close relationship. Curr. Opin. Microbiol. *16*, 112–117.

Merino, E., and Yanofsky, C. (2005). Transcription attenuation: a highly conserved regulatory strategy used by bacteria. Trends Genet. *21*, 260–264.

Miller, M.J. (1987). Sensitivity of RNA synthesis to actinomycin D inhibition is dependent on the frequency of transcription: a mathematical model. J. Theor. Biol. *129*, 289–299.

Miller, O.L., Jr., Hamkalo, B.A., and Thomas, C.A., Jr. (1970). Visualization of bacterial genes in action. Science *169*, 392–395.

Mitra, A., and Nagaraja, V. (2012). Under-representation of intrinsic terminators across bacterial genomic islands: rho as a principal regulator of xenogenic DNA expression. Gene *508*, 221–228.

Mondal, S., Yakhnin, A.V., Sebastian, A., Albert, I., and Babitzke, P. (2016). NusA-dependent transcription termination prevents misregulation of global gene expression. Nat. Microbiol. *1*, 15007.

Naville, M., and Gautheret, D. (2009). Transcription attenuation in bacteria: theme and variations. Brief Funct. Genom. Proteom. *8*, 482–492.

Newton, W.A., Beckwith, J.R., Zipser, D., and Brenner, S. (1965). Nonsense mutants and polarity in the lac operon of *Escherichia coli*. J. Mol. Biol. *14*, 290–296.

O'Reilly, F.J., Xue, L., Graziadei, A., Sinn, L., Lenz, S., Tegunov, D., Blötz, C., Singh, N., Hagen, W.J.H., Cramer, P., et al. (2020). In-cell architecture of an actively transcribing-translating expressome. Science *369*, 554–557.

Pollock, M.R. (1963). The differential effect of actinomycin D on the biosynthesis of enzymes in *Bacillus subtilis* and *Bacillus cereus*. Biochim. Biophys. Acta. *76*, 80–93.

Proshkin, S., Rahmouni, A.R., Mironov, A., and Nudler, E. (2010). Cooperation between translating ribosomes and RNA polymerase in transcription elongation. Science *328*, 504–508.

Quirk, P.G., Dunkley, E.A., Lee, P., and Krulwich, T.A. (1993). Identification of a putative *Bacillus subtilis* rho gene. J. Bacteriol. *175*, 8053.

Ray-Soni, A., Bellecourt, M.J., and Landick, R. (2016). Mechanisms of bacterial transcription termination: all good things must end. Annu. Rev. Biochem. *85*, 319–347.

Richardson, J.P. (1991). Preventing the synthesis of unused transcripts by Rho factor. Cell *64*, 1047–1049.

Richardson, J.P. (2003). Loading Rho to terminate transcription. Cell *114*, 157–159.

Rui, L., Qing, Z., Junbai, L., and Hualin, S. (2016). Effects of cooperation between translating ribosome and RNA polymerase on termination efficiency of the Rho-independent terminator. Nucleic Acids Res. 2554–2563.

Sá-Nogueira, I., Nogueira, T.V., Soares, S., and Lencastre, H.D. (1997). The *Bacillus subtilis* L-arabinose (ara) operon: nucleotide sequence, genetic organization and expression. Microbiology *143* (Pt 3), 957–969.

Santangelo, T.J., and Roberts, J.W. (2004). Forward translocation is the natural pathway of RNA release at an intrinsic terminator. Mol. Cell *14*, 117–126.

Saxena, S., Myka, K.K., Washburn, R., Costantino, N., Court, D.L., and Gottesman, M.E. (2018). *Escherichia coli* transcription factor NusG binds to 70S ribosomes. Mol. Microbiol. *108*, 495–504.

Schleif, R., Hess, W., Finkelstein, S., and Ellis, D. (1973). Induction kinetics of the L-arabinose operon of *Escherichia coli*. J. Bacteriol. *115*, 9–14.

Seo, H.S., Abedin, S., Kamp, D., Wilson, D.N., Nierhaus, K.H., and Cooperman, B.S. (2006). EF-G-dependent GTPase on the ribosome. conformational change and fusidic acid inhibition. Biochemistry *45*, 2504–2514.

Sikova, M., Wiedermannova, J., Prevorovsky, M., Barvik, I., Sudzinova, P., Kofronova, O., Benada, O., Sanderova, H., Condon, C., and Krasny, L. (2020). The torpedo effect in *Bacillus subtilis*: RNase J1 resolves stalled transcription complexes. EMBO J. *39*, e102500.

Turnbough, C.L. (2019). Regulation of bacterial gene expression by transcription attenuation. Microbiol. Mol. Biol. Rev. *83*, e00019–00019.

Van Dijl, J.M., and Hecker, M. (2013). *Bacillus subtilis*: from soil bacterium to super-secreting cell factory. Microb. Cell Fact. *12*, 3.

Vladimir, B., Pierre, N., Aleksandra, G.M., Olivier, D., Sandrine, A., Anne, A., Cyprien, G., Francis, R., Jacek, B., and Stéphane, A. (2017). Termination factor Rho: from the control of pervasive transcription to cell fate determination in *Bacillus subtilis*. PLoS Genet. *13*, e1006909.

Vogel, U., and Jensen, K.F. (1994a). Effects of guanosine 3′,5′-bisdiphosphate (ppGpp) on rate of transcription elongation in isoleucine-starved *Escherichia coli*. J. Biol. Chem. *269*, 16236–16241.

Vogel, U., and Jensen, K.F. (1994b). The RNA chain elongation rate in *Escherichia coli* depends on the growth rate. J. Bacteriol. *176*, 2807–2813.

Vogel, U., Sorensen, M., Pedersen, S., Jensen, K.F., and Kilstrup, M. (1992). Decreasing transcription elongation rate in *Escherichia coli* exposed to amino acid starvation. Mol. Microbiol. *6*, 2191–2200.

Wang, C., Molodtsov, V., Firlar, E., Kaelber, J.T., Blaha, G., Su, M., and Ebright, R.H. (2020). Structural basis of transcription-translation coupling. Science *369*, 1359–1365.

Webster, M.W., Takacs, M., Zhu, C., Vidmar, V., Eduljee, A., Abdelkareem, M.m., and Weixlbaumer, A. (2020). Structural basis of transcription-translation coupling and collision in bacteria. Science *369*, 1355–1359.

Winkler, W.C., and Breaker, R.R. (2005). Regulation of bacterial gene expression by riboswitches. Ann. Rev. Microbiol. *59*, 487.

Yakhnin, A.V., FitzGerald, P.C., McIntosh, C., Yakhnin, H., Kireeva, M., Turek-Herman, J., Mandell, Z.F., Kashlev, M., and Babitzke, P. (2020). NusG controls transcription pausing and RNA polymerase translocation throughout the *Bacillus subtilis* genome. Proc. Natl. Acad. Sci. U S A. *117*, 21628–21636.

Yakhnin, H., Babiarz, J.E., Yakhnin, A.V., and Babitzke, P. (2001). Expression of the *Bacillus subtilis* trpEDCFBA operon is Influenced by translational coupling and rho termination factor. J. Bacteriol. *183*, 5918–5926.

Yang, J., Han, Y.H., Im, J., and Seo, S.W. (2021). Synthetic protein quality control to enhance full-length translation in bacteria. Nat. Chem. Biol. *17*, 421–427.

Zhou, Y., Navaroli, D.M., Enuameh, M.S., and Martin, C.T. (2007). Dissociation of halted T7 RNA polymerase elongation complexes proceeds via a forward-translocation mechanism. Proc. Natl. Acad. Sci. USA *104*, 10352–10357.

Zhu, M., Mori, M., Hwa, T., and Dai, X. (2019). Disruption of transcription-translation coordination in *Escherichia coli* leads to premature transcriptional termination. Nat. Microbiol. *4*, 2347–2356.

STAR★METHODS

KEY RESOURCES TABLE

REAGENT or RESOURCE	SOURCE	IDENTIFIER
Bacterial and virus strains		
Bacillus subtilis 168	Professor Jianhua Zhang	N/A
Bacillus subtilis rho-null strain	This study	N/A
Bacillus subtilis rnjA-null strain	This study	N/A
Bacillus subtilis greA-null strain	This study	N/A
Bacillus subtilis PxylA-lacZ strain	This study	N/A
Bacillus subtilis PxylA-lacZ-TAA strain	This study	N/A
Chemicals, peptides, and recombinant proteins		
KH_2PO_4	Aladdin (Shanghai)	CAS: 7778-77-0
K_2HPO_4	Aladdin (Shanghai)	CAS: 7758-11-4
$MnSO_4 \cdot 4H_2O$	Macklin	CAS: 10101-68-5
$MgSO_4 \cdot 7H_2O$	Aladdin (Shanghai)	CAS: 10034-99-8
$ZnCl_2$	Macklin	CAS: 7646-85-7
Tryptophan	Aladdin (Shanghai)	CAS: 73-22-3
ferric ammonium citrate	Aladdin (Shanghai)	CAS: 1185-57-5
NH_4Cl	Sigma	G5767
Glucose	Sigma	213330
Glycerol	Aladdin (Shanghai)	CAS: 56-81-5
Fructose	Aladdin (Shanghai)	CAS: 57-48-7
Mannose	Aladdin (Shanghai)	CAS: 3458-28-4
casamino acid	Aladdin (Shanghai)	CAS: 65072-00-6
LB broth	Coolaber (Beijing)	PM0010
KNO3	Aladdin (Shanghai)	CAS: 7757-79-1
fusidic acid	Aladdin (Shanghai)	F134821
6-azauracil	Aladdin (Shanghai)	A124269
Actinomycin D	GLPBIO	GC16866
4-methylumbelliferyl-D-galactopyranoside (MUG)	Aladdin (Shanghai)	CAS: 6160-78-7
Chloramphenicol	Coolaber (Beijing)	CC3451
Erythromycin	Coolaber (Beijing)	CE5091
Spectinomycin	Coolaber (Beijing)	CS10421
Critical commercial assays		
Golden Green high-fidelity PCR mix	Tsingke Biotech	TSE101
T3 super PCR mix	Tsingke Biotech	TSE030
Total RNA extraction kit	TianGen	DP430
First-strand cDNA synthesis reverse transcriptase kit	TianGen	KR118
Plasmid extraction kit	TianGen	DP103
Bacterial genome extraction kit	TianGen	DP302
DNA purification kit	TianGen	DP209
PowerUp SYBR green Master mix	Thermo Fisher	Lot # 01000432
Super-premix SYBR green Plus kit	Yeasen Biotech	11201ES08

(*Continued on next page*)

Continued

REAGENT or RESOURCE	SOURCE	IDENTIFIER
Oligonucleotides		
P297-F/R	Tsingke Biotech	N/A
P898-F/R	Tsingke Biotech	N/A
P1578-F/R	Tsingke Biotech	N/A
P3105-F/R	Tsingke Biotech	N/A
Ara130-F/R	Tsingke Biotech	N/A
Ara1477-F/R	Tsingke Biotech	N/A
Ara3141-F/R	Tsingke Biotech	N/A
Mtl117-F/R	Tsingke Biotech	N/A
Mtl2926-F/R	Tsingke Biotech	N/A
Xyn162-F/R	Tsingke Biotech	N/A
Xyn2727-F/R	Tsingke Biotech	N/A
Recombinant DNA		
pAX01 integration vector	Professor Zheming Zhou	N/A
pDG1730 integration vector	Professor Ming Sun	N/A

RESOURCE AVAILABILITY

Lead contact

Further information and requests for materials should be directed to and will be fulfilled by the lead contact, Xiongfeng Dai (daixiongfeng@mail.ccnu.edu.cn) upon reasonable request.

Material availability

This study did not generate unique reagents.

Data and code availability

All related data are provided in the article and any further details is available from the lead contact upon reasonable request.

This paper does not report original code.

Any additional information required to reanalyze the data reported in this paper is available from the lead contact upon reasonable request.

EXPERIMENTAL MODEL AND SUBJECT DETAILS

Wild type *Bacillus subtilis* 168 strain and its derivatives were used in this study. For all related experiments, we always prepared fresh LB plates of *B. subtilis* cells (from the glycerol stock of −80°C freezer) as the starting material.

METHODS DETAILS

Strains

All the strains used in this study were derivatives of *Bacillus subtilis* 168 strain (Burkholder and Giles, 1947).

To construct an inducible *lacZ* reporter strain of *B. subtilis*, the *lacZ* gene from *E. coli* K-12 strain was inserted into the BamHI site of the pAX01 vector (with erythromycin resistance marker, *ermR*) (Härtl et al., 2001), which bears the xylose-inducible *xylR-PxylA* cassette, generating pAX01-*lacZ* vector. The pAX01-*lacZ* vector was directly transformed into *B. subtilis* 168 strain so that the *xylA-PxylA-lacZ* cassette was integrated into the *B. subtilis* genome. In the case of nonsense mutation, the coding sequence of the 154th residues of *lacZ*, "TGG", was mutated to a stop codon "TAA" by PCR-mediated point mutation using pAX01-*lacZ* as the template (Golden Green high-fidelity PCR mix from Tsingke Biotech, Beijing). The

resultant vector, pAX01-*lacZ*-null, was also transformed into *B. subtilis* 168 strain to obtain the nonsense-mutated *B. subtilis lacZ*-null strain.

To make a *rho*-null strain, a ~600 bp intragenic region of *rho* gene of *B. subtilis* was inserted into a pUC19-derived vector (with chloramphenicol resistance marker, *catR*) and integrated into the *rho* locus of *B. subtilis* 168 strain by Campbell single-crossover integration. In such case, the ORF of the native *rho* gene was disrupted by the insertion of the vector. To make the *rnjA*-null and *greA*-null strains, the flanking regions (including both upstream and downstream part) of *rnjA* and *greA* in the genome of *B. subtilis* were PCR amplified and placed at the flanking regions of the spectinomycin resistance marker (*specR*) in the integration vector, pDG1730(Guérout-Fleury et al., 1996), to replace its original *amyE* regions and further transformed into the *B. subtilis* so that the native *rnjA* and *greA* locus were replaced by *specR*.

Medium

Growth media used in this study were based on C-minimal medium with slight modifications (Commichau et al., 2008). The medium contained 4 g/L KH_2PO_4, 16 g/L K_2HPO_4, 2.32 mg/L $MnSO_4{\cdot}4H_2O$, 0.123 g/L $MgSO_4{\cdot}7H_2O$, 12.5 μM $ZnCl_2$, 50 mg/L tryptophan, and 22 mg/L ferric ammonium citrate. 20 mM NH_4Cl was used as the nitrogen source, with exception to fructose plus nitrate medium, where 20 mM KNO_3 was used as the nitrogen source. Carbon sources included 0.4% (v/v) glycerol, 0.4% (w/v) sorbitol, 0.2% (w/v) mannose, and 0.4% fructose. In addition, glycerol plus casamino acid medium (gly + cAA) contains 0.3% (w/v) casamino acids. Fusidic acid and 6-azauracil were used at a concentration of 0.2 μg/mL and 500 μg/mL, respectively.

Cell growth

Cell growth was performed in a 37°C air bath shaker shaking at 200 rpm, with exception to the case of low temperature in which 25°C was used. A standard procedure of culturing *B. subtilis* contained three steps: seed culture, pre-culture, and the final experimental culture. Cells from a fresh colony were first inoculated into LB broth and grew for several hours, as the seed culture. The seed culture was then transferred to the minimal medium (identical to the final experimental culture) and grew overnight as pre-culture. On the next day, precultures was transferred to a fresh minimal medium at an initial OD_{600}~0.02, and this was the final experimental culture. 5-8 OD_{600} data points during exponential stage (usually at the OD_{600} range of 0.08–0.6) were measured by a Thermo Sci Genesys 30 spectrophotometer to obtain an exponential growth curve from which the growth rate was calculated. For the fusidic acid study, 0.2 μg/mL fusidic acid was supplemented to the final experimental culture at OD_{600} ~0.05. The cell culture was adapted for additional two generations before reaching a stable exponential growth stage. For the 6-azauracil (6-aza) study, 500 μg/mL 6-aza was supplemented to the exponential growing culture at OD_{600}~0.25. The cell culture was further incubated for 1 h before performing transcription kinetics measurement.

Measurement of transcription kinetics

The protocol of transcription kinetics measurement was modified from the qRT-PCR method that established before (Johnson et al., 2020; Zhu et al., 2019). 1% xylose and 1% arabinose were supplemented to the exponentially growing *B. subtilis lacZ* reporter strain (OD_{600}~0.4) to induce the expression of *PxylA-lacZ* and the native *araAB* operon, respectively. 1% mannitol and 1% xylose were used to induce the expression of the native *mtlAFD* and *xynPB* operon, respectively. Immediately after inducer addition, 0.8 mL cell culture was withdrawn at a 10-20 s interval (depends on the exact growth condition) and transferred to 0.9 mL pre-chilled stop solution (60% ethanol, 2% phenol and 10 mM EDTA). Considering the thick cell wall structure of gram-positive bacteria, the stop solution also contained 10 μg/mL actinomycin D (GLPBIO), a strong blocker of transcription elongation, to ensure the immediate arrest of cellular RNA transcription(Levinthal and Higa, 1962; Pollock, 1963). Cells were pelleted at 4°C at 12000 rpm for 2 min and flash frozen by liquid nitrogen (if not immediately used for RNA extraction). Cell pellets could be stored at −80°C for a few days before RNA extraction. For RNA extraction, cell pellets were first lysed by 10 mg/mL lysozymes for 10 min at room temperature. Total cellular RNA was then extracted using a bacterial total RNA extraction kit (TianGen Biotech, Beijing). Note that during RNA extraction, the cellular DNA was removed by Dnase I. For cDNA synthesis (cDNA), 0.5 to 2 μg total cellular RNA was used with a first-strand cDNA synthesis reverse transcriptase kit (TianGen). During cDNA synthesis, a second type of Dnase, gDnase (genomic deoxyribonuclease), was added to ensure the complete elimination of genome contamination. The real time qRT-PCR was performed using either the PowerUp SYBR green Master mix (Thermo fisher) or Super-premix SYBR green Plus kit (Yeasen Biotech) with the ABI QuantStudio 3 real-time

Thermocycler. The PCR reaction procedure for thermo fisher reagents was as follows: 50°C for 2 min, 95°C for 2 min, followed by 40 cycles of 95°C for 15 s and 60°C for 1 min. The specificity of the primers is confirmed by single-peak melting curve of qPCR process. The mRNA abundance of a sample taken immediately after inducer addition (referred to as 'basal sample'), M(0), was set as '1'. The relative mRNA abundance at each time point, M(t), equals to $2^{Ct(0)-Ct(t)}$. The mRNA abundance was plotted with time to obtain the transcription kinetics of each mRNA sub-regions, including head region, middle region and tail region (detected by different pairs of qRT-PCR primers). For data of each pair of primers, the linear range of the transcription kinetics data was fit with a linear line, being expressed as $y = a \times x - b$, where "a" (the slope of the linear line) denotes the relative mRNA accumulation rate of each sub-regions. The transcription time of each mRNA sub-region, namely T_{head}, T_{mid}, T_{tail}, equals to (1 + b)/a since "1" is the basal line value before mRNA induction. The transcription elongation rates of *lacZ* and *araAB* mRNA equaled to 2808/(T_{tail}-T_{head}) and 3011/(T_{tail}-T_{head}), respectively, where 2808 and 3011 denote the distances (nt) between the tail region and head region of *lacZ* and *araAB* mRNA, respectively.

Measurement of mRNA degradation kinetics

B. subtilis lacZ reporter strain was first exponentially cultured to OD_{600}~0.4 in cAA medium or fructose plus nitrate medium (supplemented with 0.5% xylose or 0.5% arabinose). At time zero, 20 μg/mL actinomycin D (GLPBIO) were supplemented to completely block the cellular transcription process of *B. subtilis*(Levinthal and Higa, 1962). 0.8 mL cell culture was then withdrawn at a 1 min interval and transferred to 0.9 mL pre-chilled stop solution (60% ethanol, 2% phenol and 10 mM EDTA). Cell samples were then subject to RNA extraction and qRT-PCR as detailed in the section of measurement of transcription kinetics. Different sets of qRT-PCR probes were used to detect different sub-regions of *lacZ* and *araAB* mRNA. The relative abundances of *lacZ* and *araAB* mRNA were plotted with time to obtain the exponential mRNA degradation curve (see Figure S3) from which mRNA decay rates and half-lives could be calculated.

Measurement of translation kinetics

Measurement of the translation elongation rate was based on the classical LacZ induction assay, initially developed by Schelif *et al*(Schleif et al., 1973) and extensively used in recent studies(Dai et al., 2016; Iyer et al., 2018; Johnson et al., 2020; Zhu et al., 2019). 1% xylose was supplemented to the exponentially growing *B. subtilis lacZ* reporter strain (OD_{600}~0.4) to induce the expression of *PxylA-lacZ*. Immediately after induction, at 15-s to 30-s intervals (depending on the growth condition), aliquots of 400-μL culture were transferred into pre-chilled microfuge tubes (Nest Biotech) containing 10-μL chloramphenicol (34 mg/mL) for a total of 18–20 time points. Samples were flash frozen at liquid nitrogen and stored at −80°C prior to LacZ assay. Measurement of LacZ activity was based on a sensitive fluorescence substrate 4-methylumbelliferyl-D-galactopyranoside (MUG). Briefly, 100-μL cell sample was added to 400-μL Z-buffer and warmed at 37°C for 10 min 50 μL of 2 mg/mL MUG was added and the reaction mixtures were incubated for 0.5–1 h. The reaction was stopped by 250 μL of 1 M Na_2CO_3. The fluorescence intensity was measured with a microplate reader (360 nm excitation filter, 460 nm emission filters). LacZ induction curve was made by plotting the LacZ activity against the induction time and further analyzed using a square root plot (Schleif plot) to obtain the lag time for the synthesis of the first LacZ molecule (T_{first}). The translation elongation rate equals to 1024/(T_{first}-T_{ini}), where T_{ini} denotes the time cost of initiation steps including the penetration of xylose into cells, XylR repressor depression and transcription initiation. T_{ini} was obtained by analyzing the induction kinetics of head region of *lacZ* mRNA. T_{ini} was relatively constant at ~20 s and ~45 s under 37°C and 25°C, respectively.

QUANTIFICATION AND STATISTICAL ANALYSIS

The slope of the linear mRNA induction curve was analyzed by GraphPad Prism 8 software using linear fit.